# Labeling Diversity for 2 × 2 WLAN Coded-Cooperative Networks

*Saqib EJAZ[1], FengFan YANG[1], HongJun XU[2]*

[1]College of Electronic and Information Engineering, Nanjing University of Aeronautics and Astronautics,
29 Yudao Street, 210016, Nanjing, China
[2]School of Engineering, University of KwaZulu-Natal, King George V Avenue, Durban, 4041, South Africa

saqib.ejaz@foxmail.com, yffee@nuaa.edu.cn, and xuh@ukzn.ac.za

**Abstract.** *Labeling diversity is an efficient technique recently proposed in the literature and aims to improve the Bit Error Rate (BER) performance of Wireless Local Area Network (WLAN) systems with two transmit and two receive antennas without increasing the transmit power and bandwidth requirements. In this paper, we employ labeling diversity with different space-time channel codes such as convolutional, turbo and Low Density Parity Check (LDPC) for both point-to-point and coded-cooperative communication scenarios. Joint iterative decoding schemes for distributed turbo and LDPC codes are also presented. BER performance bounds at an Error Floor (EF) region are derived and verified with the help of numerical simulations for both cooperative and non-cooperative schemes. Numerical simulations show that the coded-cooperative schemes with labeling diversity achieve better BER performances and use of labeling diversity at the source node significantly lowers relay outage probability and hence the overall BER performance of the coded-cooperative scheme is improved manifolds.*

## Keywords

Alamouti, boosted scheme, coded-cooperation, joint decoding, labeling diversity, LDPC, space-time, turbo, WLAN

## 1. Introduction

The concept of cooperative diversity traces back to the work of Van der Meulen [1] and has proven to be an effective way to minimize the channel impairments on the transmission of a wireless signal. Usually, a typical cooperative system consists of one source *S*, one relay *R* and a common destination *D*. This relay *R* terminal has been used in different configurations such as Amplify and Forward (A-F), Estimate and Forward (E-F), and Decode and Forward (D-F) [2]. In view of mobile communications, the relay can be another user (mobile station) and can share its antenna and resources with the source (mobile station) to make a virtual antenna array and provide spatial/path diversity to the destination (usually the base station) [3]. The concept of co-

operative diversity opened a gateway for the mobile devices to exploit spatial diversity without using an actual Multiple-Input and Multiple-Output (MIMO) [4].

Coded-cooperative diversity between the two users was introduced in [5]. It was the merger of existing channel coding techniques with the cooperative schemes. In a coded-cooperation, the source and the relay terminal jointly construct more powerful (in terms of error correction) channel code at the destination. Joint decoding scheme is then established at the destination to recover the information transmitted at the source. Different channel codes such as convolution codes [6], turbo codes [7], [8], [9], Low Density Parity Check (LDPC) [10], [11], and recently polar codes [12], [13] have been utilized in the coded cooperative schemes.

However, apart from many advantages offered by the coded-cooperative communication, one of the major drawbacks is the poor bandwidth efficiency as most of the proposed coded-cooperative schemes are designed for Binary Phase Shift Keying (BPSK) modulation. This issue can be resolved by using high order modulation schemes such as 4-QAM, 16-QAM or more higher order of Quadrature Amplitude Modulation (QAM) as in case of most practical scenarios [14]. However, as modulation order increases the BER performance significantly drops. Therefore, the concept Bit-Interleaved Coded-Modulation (BICM) evolved, which brings synergy between the code design and the modulation techniques [15].

It is a known fact that the Bit Error Rate (BER) performance of Bit-Interleaved Coded Modulation (BICM) depends significantly on the labeling map and is further improved with the help of iterative decoding [16], [17], [18]. However, the cost of improved performance is increased latency of the communication system, which may be one of the critical factors in some applications such as live telemetry and video broadcasts in satellite communication systems [19]. A map is a rule according to which the encoded binary bits are assigned symbols from the set of constellation χ. The idea of the optimal labeling for iteratively decoded bit-interleaved space-time coded modulation was presented in [20]. Recently, a novel diversity scheme known as *Labeling Diversity* has been introduced in the literature for Bit-Interleaved Space-Time Coded Modulation with It-

erative Decoding (BI-StCM-ID) systems for two transmit and two receive antennas for WLAN applications [21], [22]. Until now, labeling diversity is proposed only for 16-QAM modulation, however the general idea of labeling diversity can be extended to other high order modulation schemes as well. Labeling diversity has shown promising BER performance gains over the systems without labeling diversity, and also lowers the Error Floor (EF) region by ensuring error free feedback during the iterative process [21]. The fundamental principle of labeling diversity is to apply two different labeling maps for the two adjacent spatial streams of the transmitter. In [20], the BI-StCM-ID was compared with the Boosted scheme [23] equipped with the labeling diversity and in this paper it is referred to as Bit-Interleaved Boosted Coded Modulation with Iterative Decoding (BI-BoCM-ID). Moreover, in [18], for the non-cooperative schemes, various analysis such as Extrinsic Information Transfer (EXIT) chart, distance spectrum, asymptotic gain and Monte Carlo simulations proved the supremacy of the BI-BoCM-ID scheme over BI-StCM-ID (without any labeling diversity).

In this paper, we use the Boosted scheme (employing labeling diversity) for coded-cooperative communication systems, but without an iterative decoding to reduce the complexity of the receiver. To use the Boosted scheme in a coded-cooperative scenario, we consider two channel codes such as the turbo and LDPC codes as suitable candidates for the coded-cooperative diversity scheme [10]. The natural extension of the BI-StCM scheme, which uses only one convolution code is a Bit-Interleaved Space time Turbo-Coded Modulation (BI-StTCM). Ordinary Bit Interleaved Turbo Coded Modulation (BI-TCM) is a well-established bandwidth and power efficient coding technique [24], which has shown to achieve BER performance very near to the capacity limit over both Additive White Gaussian Noise (AWGN) and Rayleigh fading channels [25]. Its descendant for multi-antenna systems BI-StTCM is also well known and efficient approach [26]. BICM for LDPC codes is discussed in [27], [28], [29] for 16-QAM and even for high order of modulation. Space-time LDPC codes are suggested in [30] for orthogonal frequency-division multiplexing (OFDM) system with multiple transmitter and receiver antennas over correlated frequency-and time-selective fading channels.

In the remainder of this paper, the Boosted scheme employing distributed turbo codes and labeling diversity is referred to as Bit-Interleaved Boosted Distributed Turbo Coded Modulation (BI-BoDTCM) and Boosted scheme employing distributed LDPC codes and labeling diversity is referred to as Bit-Interleaved Boosted Distributed LDPC Coded Modulation (BI-BoDLCM). For a benchmark reference to our proposed BI-BoDTCM and BI-BoDLCM schemes, we consider Bit-Interleaved Space-time Distributed Turbo Coded Modulation (BI-StDTCM) and Bit-Interleaved Space-time Distributed LDPC Coded Modulation (BI-StDLCM) schemes, respectively. The receiver for BI-BoCM scheme and the BI-StCM are identical and so

are the receivers for BI-BoDTCM/BI-BoDLCM and BI-StDTCM/BI-StDLCM.

The major contributions of this paper can be summarized as follows:

- To the best of our knowledge, labeling diversity is used for the first time in conjunction with space-time turbo and LDPC codes in a non-iterative manner.
- Performance analysis of the non-cooperative Boosted transmission scheme (BI-BoCM) is extended to the coded-cooperative Boosted transmission scheme (BI-BoDTCM).
- Derived theoretical BER performance bounds at Error Floor (EF) region are verified using numerical simulations.
- Coded-cooperative scenarios are presented not only for ideal conditions but also for non-ideal (practical) scenarios.

The remainder of this paper is organized as follows: Section 2 briefly explains the generalized three-terminal space-time coded-cooperation. Coded-cooperative encoding schemes are discussed in Section 3. Section 4 gives brief description of space-time diversity schemes considered in this paper. In Section 5, a brief overview and asymptotic gain due to the labeling diversity is discussed. Performance analysis for non-cooperative and coded-cooperative schemes is presented in Section 6. Joint iterative decoding schemes for space-time turbo and LDPC codes are discussed in Section 7. Monte-Carlo simulations are performed and different simulations scenarios are presented in Section 8. Finally, Section 9 concludes the article.

## 2. Generalized Space-time Coded-Cooperation

The generalized three-terminal space-time coded-cooperative communication system is shown in Fig. 1. The system topology is based on the famous idea of Van der Meulen three-terminal communication [1], where the three terminals are source $S$, relay $R$, and the destination $D$. The end-to-end transmission of information transmitted at the source takes two time slots and the communication takes place in half-duplex mode. Each communication node has two antennas to transmit and receive the data with an assumption that antennas have enough separation between them to avoid any mutual interference. During the first time slot, also referred to as broadcast phase, the information vector $\mathbf{m}_1$ is encoded by a channel code $C_1$, which may be any channel code such as convolutional, turbo or LDPC code. The encoded signal is then passed to the space-time diversity block as illustrated in Fig. 1, which modulates the binary encoded signal to space-time codeword $\mathbf{X}_S$ and broadcasts over the radio frequency (RF) channel to the both relay and the destination. The details of this space-time diversity block are presented in Section 4. During the first time slot,
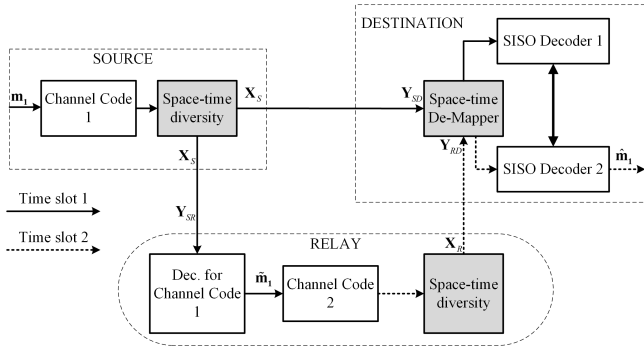
**Fig. 1.** Generalized block diagram of distributed space-time coded-cooperative scheme with reference to time.

the signal received at the relay is modeled as,

$$\mathbf{Y}_{S-R} = \mathbf{X}_S \mathbf{H}_{S-R} + \mathbf{N}_{S-R} \qquad (1)$$

where $\mathbf{X}_S$ is a $T \times N_t$ matrix, $T$ is the number of time slots for transmitting one space-time codeword $\mathbf{X}_S$, $N_t$ and $N_r$ are the number of transmit and receive antennas, respectively, $\mathbf{H}_{S-R}$ is $N_t \times N_r$ channel matrix between the source and the relay nodes. In case of Rayleigh fading channel, the entries of the $\mathbf{H}_{S-R}$ matrix are independent and identically distributed (i.i.d.) complex Gaussian random variables (RVs) with zero mean and variance $1/2$ per dimension, and $\mathbf{N}_{S-R}$ is the $T \times N_r$ noise matrix whose entries are modeled as i.i.d. complex Gaussian RVs with zero mean and variance $N_0/2$ per dimension. For a fast-fading channel, $\mathbf{H}_{S-R}$ remains constant during the transmission of one single space-time codeword $\mathbf{X}_S$ and varies independently over the transmission of the next $\mathbf{X}_S$. The received signal $\mathbf{Y}_{S-R}$ is then decoded to recover information bits $\tilde{\mathbf{m}}_1$ transmitted at the source during first time slot, where $\tilde{\mathbf{m}}_1$ may or may not be equal to $\mathbf{m}_1$ depending upon the $S - R$ link condition.

The received signal at the destination during the first time slot is given as,

$$\mathbf{Y}_{S-D} = \mathbf{X}_S \mathbf{H}_{S-D} + \mathbf{N}_{S-D} \qquad (2)$$

where $\mathbf{H}_{S-D}$ and $\mathbf{N}_{S-D}$ are the channel and the Gaussian noise matrices, respectively, and defined similarly as $\mathbf{H}_{S-R}$ and $\mathbf{N}_{S-R}$.

During the second time slot, the relay re-encodes the decoded message vector $\tilde{\mathbf{m}}_1$ using channel code $C_2$. The resultant binary codeword is then passed to the space-time diversity block, which modulates and propagates the signal $\mathbf{X}_R$ towards the destination. The signal received at the destination during the second time slot is given as,

$$\mathbf{Y}_{R-D} = \mathbf{X}_R \mathbf{H}_{R-D} + \mathbf{N}_{R-D} \qquad (3)$$

where $\mathbf{H}_{R-D}$ and $\mathbf{N}_{R-D}$ are the channel and the Gaussian noise matrices, respectively, and are defined similarly as $\mathbf{H}_{S-R}$ and $\mathbf{N}_{S-R}$.

The received signals $\mathbf{Y}_{S-D}$ and $\mathbf{Y}_{R-D}$ during each time slot are demodulated by a soft output demodulator, which generates log likelihood ratio (LLRs) for each received bit. These LLRs are then passed to the *joint* iterative decoder (in case turbo or LDPC codes are used), which then iterates for desired number of iterations and finally pass the updated LLRs to the slicer to recover the information vector as $\hat{\mathbf{m}}_1$. The term *joint* refers to the fact that the received signals $\mathbf{Y}_{S-D}$ and $\mathbf{Y}_{R-D}$ are decoded jointly instead of decoding each received signal individually. This joint decoding results in significant bit error rate (BER) performance gains [9].

The code rate at the source is defined as $R_c = K/N_1$, where $K$ is the information block size and $N_1$ is the codeword block size. The generalized overall code rate $R_c^o$ of a coded-cooperative scheme from the destination point of view is, $R_c^o = K/(N_1 + N_2)$, where $N_2$ is the codeword block size generated at the relay.

Let $\mathbf{X}$ be the set of all space-time codeword matrices generated at a transmitter (source or relay). The modulator and the space-time block code (STBC) jointly define overall one-to-one mapping rule $M : \{0,1\}^L \to \mathbf{X}$. $\forall \mathbf{X}_i \in \mathbf{X}$, where $i = \{S, R\}$ node, the corresponding $L$-tuple binary label is $M^{-1}(\mathbf{X}_i)$.

The symbol energy is normalized to unity i.e., $E_s = 1$ independent of transmit antennas $N_t$. The rate of the STBC is defined as $R_{STBC} = q/T$, where $q = N_w/\log_2(m)$, $w = 1, 2$ is the number of symbols in one transmitted frame, $m$ is the modulation order and the overall information rate of the system is $R_{overall} = mR_c^o R_{STBC}$, and the average energy per information bit is $E_b = E_s/R_{overall} = 1/R_{overall}$ [16].

## 3. Coded-Cooperative Encoding Schemes

In this section, we briefly discuss encoding configurations for channel codes $C_1$ and $C_2$ as shown in Fig. 1. Two famous channel codes such as turbo and LDPC codes are considered in this paper and their performance is analysed in conjunction with the labeling diversity.

### 3.1 Distributed Turbo Code (DTC)

In a typical distributed turbo code (DTC) scenario [9], the channel code $C_1$ used at the source shown in Fig. 1 is a recursive systematic convolutional (RSC) code, denoted as $RSC_1$. During the first time slot, $K$ information bits are encoded to $N_1$ bits at the source and after modulation broadcasted to the relay and destination. If the decoding at the relay node is successful, then the decoded information bits are interleaved by $S$−random interleaver, where $S \le \sqrt{K/2}$ and further re-encoded by a second RSC encoder $RSC_2$, assumed identical to $RSC_1$. The encoded codeword is a binary vector of length $1 \times N_2$ is then modulated and transmitted to the destination during the second time slot. The overall transmission rate from the destination point of view is $R_c^o = K/(N_1 + N_2)$.

## 3.2 Distributed LDPC Code (DLDPC)

In a typical single relay LDPC based coded-cooperation [31], at first, information vector $\mathbf{m}_1$ is encoded by the $C_1 = LDPC_S$ code to a codeword given as,

$$\mathbf{c}_1 = \left[m_1, m_2, ..., m_{N-M_1}, p_1^{(S)}, p_2^{(S)}, ..., p_{M_1}^{(S)}\right]^t \quad (4)$$

where parity-check matrix of $LDPC_S$ is given as,

$$\mathbf{H}_S = \left[\mathbf{A}_{M_1 \times (N-M_1)} \; \mathbf{D}_{M_1 \times M_1}\right]. \quad (5)$$

The codeword $\mathbf{c}_1$ is then modulated and transmitted to the both source and the relay channel. With an assumption of error free decoding at the relay, the recovered information bits are re-encoded by $C_2 = LDPC_R$, with a parity check matrix given as,

$$\mathbf{H}_R = \left[\mathbf{B}_{M_2 \times (N-M_1)} \; \mathbf{D}_{M_2 \times M_2}\right]. \quad (6)$$

From the encoded codeword $\mathbf{c}_2 = [m_1, m_2, ..., m_{N-M_1}, p_1^{(R)}, p_2^{(R)}, ..., p_{M_2}^{(R)}]^t$, only the parity-check bits $[p_1^{(R)}, p_2^{(R)}, ..., p_{M_2}^{(R)}]$ are further modulated and transmitted to the destination during the second time slot.

From the destination point of view, the overall parity-check matrix $\mathbf{H}$ has the following structure,

$$\mathbf{H} = \begin{bmatrix} \mathbf{A}_{M_1 \times (N-M_1)} & \mathbf{D}_{M_1 \times M_1} & \mathbf{0}_{M_1 \times M_2} \\ \mathbf{B}_{M_2 \times (N-M_1)} & \mathbf{0}_{M_2 \times M_1} & \mathbf{D}_{M_2 \times M_2} \end{bmatrix} \quad (7)$$

and the codeword $\mathbf{c}$ obtained at the destination is a vector of length $N + M_2$ given as,

$$\mathbf{c} = \left[m_1, m_2, ..., m_{N-M_1}, p_1^{(S)}, p_2^{(S)}, ..., p_{M_1}^{(S)}, p_1^{(R)}, p_2^{(R)}, ..., p_{M_2}^{(R)}\right]^t \quad (8)$$

where $\mathbf{Hc} = \mathbf{0}$. The Bi-layer Tanner graph [32] of an overall parity-check matrix $\mathbf{H}$ is shown in Fig. 2, where the first and second layers correspond to parity check matrices $\mathbf{H}_S$ and $\mathbf{H}_R$, respectively.
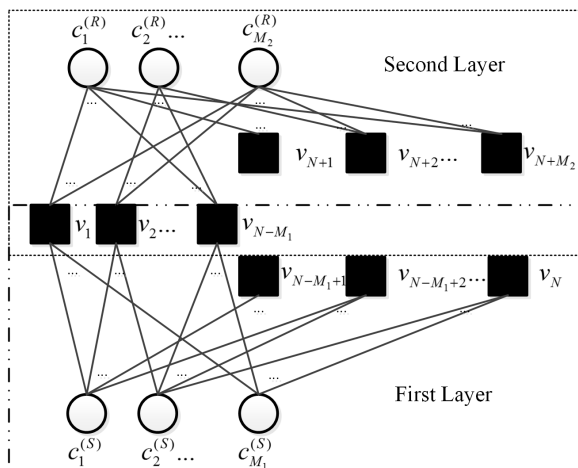


**Fig. 2.** Bi-layer Tanner graph, [32].

As shown in Fig. 2, $v_n (n = 1, 2, ..., N - M_1)$ are the common variable nodes of $\mathbf{H}_S$ and $\mathbf{H}_R$, whereas, $v_n (n = N - M_1 + 1, N - M_1 + 2, ..., N)$ are related to $\mathbf{H}_S$ and $v_n (n = N + 1, N + 2, ..., N + M_2)$ correspond to $\mathbf{H}_R$. The check nodes $c_m^{(S)} (m = 1, 2, ..., M_1)$ and $c_m^{(R)} (m = 1, 2, ..., M_2)$ are related to $\mathbf{H}_S$ and $\mathbf{H}_R$, respectively. The overall transmission rate from the destination point of view is $R_c^o = (N - M_1)/(N + M_2)$.

## 4. Space-time Diversity Schemes

### 4.1 Conventional Space-Time BICM Scheme

The conventional transmitter of a space-time bit inter-leaved coded modulation scheme referred to as BI-StCM in the rest of the paper is shown in Fig. 3.
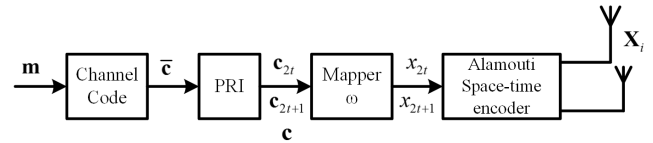


**Fig. 3.** Transmitter of BI-StCM scheme.

In this scheme, the information vector $\mathbf{m}$ is encoded by the channel code to the vector $\bar{\mathbf{c}}$, which is then bit-interleaved by a pseudo-random interleaver (PRI) and passed to the mapper $\omega$, usually the Gray labeling mapper. After mapping of binary codewords to constellation points, they are further passed to the famous Alamouti space-time encoder before their upconversion to the radio frequency. The space-time codeword $\mathbf{X}_i$ is defined as,

$$\mathbf{X}_i = \begin{bmatrix} x_{2t} & (x_{2t+1})* \\ x_{2t+1} & (-x_{2t})* \end{bmatrix} = \begin{bmatrix} \omega(\mathbf{c}_{2t}) & \omega(\mathbf{c}_{2t+1})* \\ \omega(\mathbf{c}_{2t+1}) & -\omega(\mathbf{c}_{2t})* \end{bmatrix} \quad (9)$$

where * is a complex conjugate, the rows of matrix $\mathbf{X}_i$ represent two spatial streams and columns represent time slots.

### 4.2 Boosted Scheme

It is a known fact that the BI-StCM suffers from the significant BER performance loss particularly when Gray labeling is used in both spatial streams. The improvement to BI-StCM was suggested in [18] and the novelty was to use two different labeling maps in adjacent space streams at the transmitter, as shown in Fig. 4.
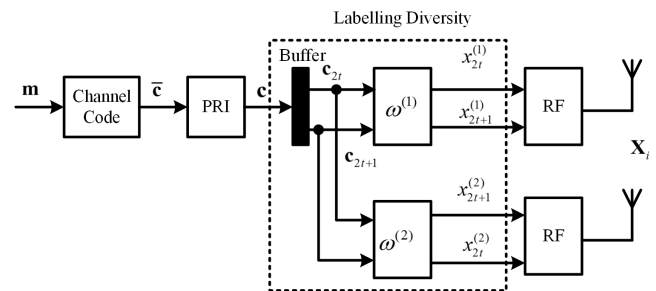


**Fig. 4.** Transmitter of a Boosted scheme.

The information sequence $\mathbf{m}$ is encoded by the channel code (convolutional encoder in [18]) to a binary encoded vector $\bar{\mathbf{c}}$, which is then passed to PRI. After bit-interleaving, the binary codeword bit train is split in two short bit-trains of equal length and passed to the two different labeling mappers i.e., $\omega^{(1)}$ and $\omega^{(2)}$. In the lower branch, the outputs $x_{2t}^{(2)}$ and $x_{2t+1}^{(2)}$ of mapper $\omega^{(2)}$ are interleaved again and passed to the space-time mapper. The space-time mapper takes two baseband signals as its input and generates a space-time codeword matrix $\mathbf{X}_i$ defined as,

$$\mathbf{X}_i = \begin{bmatrix} x_{2t}^{(1)} & x_{2t+1}^{(1)} \\ x_{2t+1}^{(2)} & x_{2t}^{(2)} \end{bmatrix} = \begin{bmatrix} \omega^{(1)}(\mathbf{c}_{2t}) & \omega^{(1)}(\mathbf{c}_{2t+1}) \\ \omega^{(2)}(\mathbf{c}_{2t+1}) & \omega^{(2)}(\mathbf{c}_{2t}) \end{bmatrix}. \quad (10)$$

The non-iterative receiver common to both of the aforementioned transmission schemes is shown in Fig. 5. For original BI-StCM and Boosted schemes, there exists a feedback path between soft-input soft-output (SISO) decoder and the soft-demodulator. However, to keep the complexity of the receiver at minimum we assume that there is no feedback path between SISO decoder and the soft demodulator.
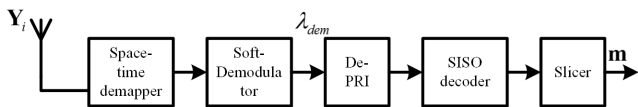


**Fig. 5.** Non-iterative receiver for BI-StCM and Boosted schemes.

The received signal $\mathbf{Y}_j$ is passed to the soft-demodulator, which generates LLRs $\lambda_{dem}$ corresponding to each received bit transmitted at the source. Next, $\lambda_{dem}$ is de-interleaved by (De-PRI) block and the LLRs are passed to the SISO decoder, whose LLRs are further passed to the slicer for making hard decisions over LLRs.

# 5. Overview of Labeling Diversity

The fundamental idea of the *labeling diversity* is to use two different labeling maps such as $\omega^{(1)}$ and $\omega^{(2)}$ for two spatial streams instead of using identical labeling maps in each spatial branch. However, search of such labeling maps or a labeling map pair is more complex and has been recently investigated in [21]. In this section, we present the coding gain achieved due to the labeling diversity. The following analysis is not new, however, it is necessary to present here to understand the magic behind the labeling diversity.

Asymptotic coding gain is greatly affected by the distance between such space-time codewords $\mathbf{X}_i$ and $\mathbf{Z}_i$ that the binary vectors assigned to them, i.e., $\mathbf{w}(\mathbf{X}_i)$ and $\mathbf{w}(\mathbf{Z}_i) \equiv \tilde{\mathbf{w}}_k(\mathbf{X}_i)$, differ exactly at one position (denoted as $k$). The $\mathcal{K}$ bit length vector $\mathbf{w}$ consists of two $\mathcal{K}/2$-bit length vectors $\mathbf{c}$ and $\mathbf{c}'$, which are mapped onto the constellation points according to the labeling maps $\omega^{(1)}$ and $\omega^{(2)}$, respectively, in two spatial streams as shown in Fig. 4.

$$\mathbf{w} = [\mathbf{c}_{1 \times \mathcal{K}/2} | \mathbf{c}'_{1 \times \mathcal{K}/2}]_{1 \times \mathcal{K}}. \quad (11)$$

To determine the symbol cost, let $\omega^{(l)}(\mathbf{c})$ be a constellation point onto which the binary vector $\mathbf{c}$ is mapped according to the labeling map $\omega^{(l)}$, where $l = 1, 2$. Using the same notational analogy $\tilde{\mathbf{w}}_k(\mathbf{X}_i)$, vector $\tilde{\mathbf{c}}_k$, differing on position $k$ from $\mathbf{c}$, is introduced. Similarly, $\tilde{\mathbf{c}}'_k$ differs from $\mathbf{c}'$. To compute the *asymptotic gain* denoted as $\psi^2$, the product of the eigenvalues (or the determinant) of matrix $\tilde{\mathbf{A}}$ must be evaluated,

$$\tilde{\mathbf{A}} = (\mathbf{X}_i - \mathbf{Z}_i)^H (\mathbf{X}_i - \mathbf{Z}_i) \quad (12)$$

where $H$ represents the Hermitian operation. For $k \leq \mathcal{K}/2$ we get,

$$\mathbf{X}_i = \begin{bmatrix} \omega^{(1)}(\mathbf{c}) & \omega^{(1)}(\mathbf{c}') \\ \omega^{(2)}(\mathbf{c}') & \omega^{(2)}(\mathbf{c}) \end{bmatrix}, \mathbf{Z}_i = \begin{bmatrix} \omega^{(1)}(\tilde{\mathbf{c}}_k) & \omega^{(1)}(\mathbf{c}') \\ \omega^{(2)}(\mathbf{c}') & \omega^{(2)}(\tilde{\mathbf{c}}_k) \end{bmatrix} \quad (13)$$

Substituting in (12) we get,

$$\tilde{\mathbf{A}} = \begin{bmatrix} |\omega^{(1)}(\mathbf{c}) - \omega^{(1)}(\tilde{\mathbf{c}}_k)|^2 & 0 \\ 0 & |\omega^{(2)}(\mathbf{c}) - \omega^{(2)}(\tilde{\mathbf{c}}_k)|^2 \end{bmatrix}. \quad (14)$$

For $k > \mathcal{K}/2$ matrix $\mathbf{X}_i$ remains unchanged, however, matrix $\mathbf{Z}_i$ is now re-defined as follows:

$$\mathbf{Z}_i = \begin{bmatrix} \omega^{(1)}(\mathbf{c}) & \omega^{(1)}(\tilde{\mathbf{c}}'_k) \\ \omega^{(2)}(\tilde{\mathbf{c}}'_k) & \omega^{(2)}(\mathbf{c}) \end{bmatrix}. \quad (15)$$

Consequently, the matrix $\tilde{\mathbf{A}}$ is,

$$\tilde{\mathbf{A}} = \begin{bmatrix} |\omega^{(2)}(\mathbf{c}') - \omega^{(2)}(\tilde{\mathbf{c}}'_k)|^2 & 0 \\ 0 & |\omega^{(1)}(\mathbf{c}') - \omega^{(1)}(\tilde{\mathbf{c}}'_k)|^2 \end{bmatrix}. \quad (16)$$

To simplify the notations, we define a variable $d^l_{(\mathbf{c}, \tilde{\mathbf{c}}_k)}$ to represent the Euclidean distance between the baseband signals $\omega^{(l)}(\mathbf{c})$ and $\omega^{(l)}(\tilde{\mathbf{c}}_k)$, into which binary vectors $\mathbf{c}$ and $\tilde{\mathbf{c}}_k$ are mapped according to the labeling rule $\omega^{(l)}$:

$$d^l_{(\mathbf{c}, \tilde{\mathbf{c}}_k)} = |\omega^{(l)}(\mathbf{c}) - \omega^{(l)}(\tilde{\mathbf{c}}_k)|^2. \quad (17)$$

The asymptotic coding gain is then written as [18],

$$\psi^2 = \left[ \frac{1}{2^{\mathcal{K}} \mathcal{K}} \sum_{\mathbf{X}} \sum_{k=1}^{\mathcal{K}} \left( \det \tilde{\mathbf{A}} \right)^{-N_r} \right]^{-1/\rho N_r} \quad (18)$$

where $d^1_{(\mathbf{c}, \tilde{\mathbf{c}}_k)} = \left| \omega^{(1)}(\mathbf{c}) - \omega^{(1)}(\tilde{\mathbf{c}}_k) \right|^2$ and $d^2_{(\mathbf{c}, \tilde{\mathbf{c}}_k)} = \left| \omega^{(2)}(\mathbf{c}) - \omega^{(2)}(\tilde{\mathbf{c}}_k) \right|^2$. The utility function $\kappa$ is mainly dependent on the Euclidean distances $d^l_{(\mathbf{c}, \tilde{\mathbf{c}}_k)}$ between the signals $x = \omega^{(l)}(\mathbf{c})$ and associated with the label $\tilde{\mathbf{c}}_k$ differing from $\mathbf{c}$ exactly in the $k$-th position. It should be noted that shorter the distance, the worse is its impact on the asymptotic coding gain. The core idea is to provide individual mappings with a different set of constellation points for any $\mathbf{c}$. This is what makes labeling diversity transmission scheme more robust as compared to the systems without labeling diversity. Each symbol (constellation point in $\chi$) from different mapping has different distance spectrum and thus suffers from different fading when propagated in the channel. This fundamental rule for labeling diversity is illustrated in Fig. 6.
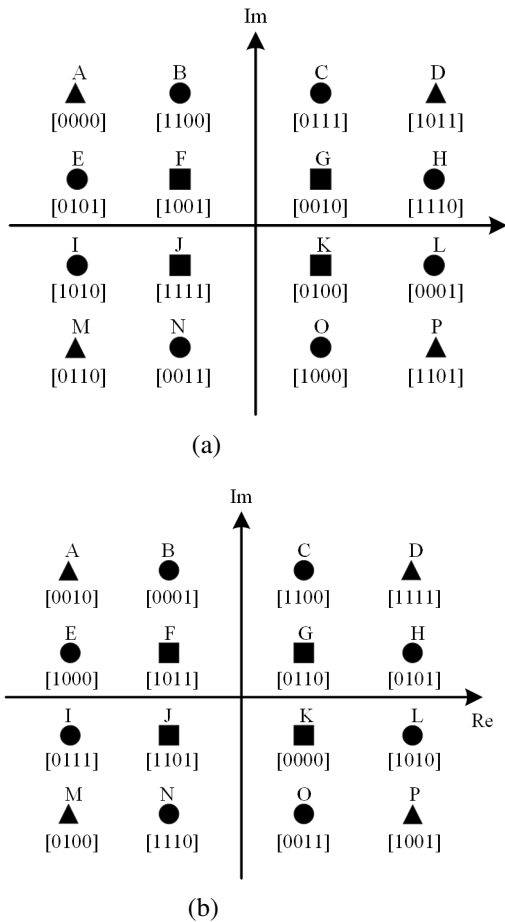
**Fig. 6.** Optimal Labeling map pair (a) Labeling map $\omega^{(1)}$ and (b) Labeling map $\omega^{(2)}$ from [21].

It can be seem from Fig. 6 that labels associated with *corner* points according to the $\omega^{(1)}$ are the most *inner* points according to the labeling map $\omega^{(2)}$ and vice versa. Another useful inference was made in [21] that assigning a new labeling map is a necessary but not sufficient condition. The relation between labelings making the *optimal pair* is more complex, since (18) has a form of the sum over $k$, therefore, all the individual distance pairs $(d^1_{(\mathbf{c},\tilde{\mathbf{c}}_k)} d^2_{(\mathbf{c},\tilde{\mathbf{c}}_k)})$ must be analyzed to achieve the optimal performance via labeling diversity. Six different optimal labeling pairs were found in [21] using the modified Binary Switching optimization Algorithm (BSA). The details of the BSA are beyond the scope of this paper, however, interested readers are referred to [21]. One of the optimal labeling pairs found in [21] is shown in Fig. 6 and in this paper, we consider this optimal labeling map pair to provide labeling diversity.

# 6. Asymptotic Performance Analysis

In this section, we present the asymptotic performance analysis of space-time BICM schemes. Firstly, we consider non-cooperative scenario and later we extend our analysis to coded-cooperative scheme.

## 6.1 Non-Cooperative Labeling Diversity Scheme, BI-BoCM

The following analysis is valid for convolutional as well as space-time distributed turbo codes. Assuming uniform random interleaving, the union bound estimate of the probability of bit error is given as,

$$P_b \leq \frac{1}{k} \sum_{d=d_f}^{\infty} W_I(d) p(d,\chi,M) \tag{19}$$

where $d_f$ is the minimum free distance of the turbo code, $W_I(d)$ is the total input weight of error events at Hamming distance $d$, and $p(d,\chi,M)$ is the pairwise error probability (PEP) and is a function of the Hamming distance $d$, the signal constellation $\chi$ and the mapping rule $M$. At high SNR, the iterative turbo decoding shows a phenomena well known as error floor (EF) and the BER performance in this region is referred to as asymptotic BER performance. To determine the asymptotic BER performance, some of the error items in the $p(d,\chi,M)$ can be expurgated to achieve the error-free feedback performance and is given as [16],

$$p_{UB}(d,\chi,M) \leq \left[ \frac{1}{2^K K} \sum_{k=1}^{K} \sum_{b=0}^{1} \sum_{\mathbf{X}_i \in \chi_b^k} \sum_{\mathbf{Z}_i \in \chi_{\bar{b}}^k} \min_s \Phi_{\Delta(\mathbf{X}_i,\mathbf{Z}_i)}(s) \right]^d. \tag{20}$$

For a non-cooperative scenario, $i = S$, and $d = d_1$ is the Hamming distance of the codeword generated at the source node. Then, (20) can be written as,

$$p_{UB}^{S-D}(d_1,\chi,M) \leq \left[ \frac{1}{2^K K} \sum_{k=1}^{K} \sum_{b=0}^{1} \sum_{\mathbf{X}_S \in \chi_b^k} \sum_{\mathbf{Z}_S \in \chi_{\bar{b}}^k} \min_s \Phi_{\Delta(\mathbf{X}_S,\mathbf{Z}_S)}(s) \right]^{d_1} \tag{21}$$

where $\mathbf{X}_S$ is a transmitted codeword at the source and $\mathbf{Z}_S$ is the received codeword with errors at the destination during the first time slot, and $\Phi_{\Delta(\mathbf{X}_i,\mathbf{Z}_i)}(s)$ is the Laplace transform of the pdf of the difference metric $\Delta(\mathbf{X}_S,\mathbf{Z}_S)$ between the two space-time codewords defined as,

$$\Delta(\mathbf{X}_S,\mathbf{Z}_S) = ||\mathbf{Y}_S - \mathbf{Z}_S \mathbf{H}_{S-D}||_F^2 - ||\mathbf{Y}_S - \mathbf{X}_S \mathbf{H}_{S-D}||_F^2 \tag{22}$$

where the subscript $F$ represents the Frobenius norm. Further, the Chernoff bound for $\Phi_{\Delta(\mathbf{X}_i,\mathbf{Z}_i)}(s)$ is given as [16],

$$\min_s \Phi_{\Delta(\mathbf{X}_S,\mathbf{Z}_S)}(s) = \left[ \prod_{y=1}^{\rho} \left( 1 + \frac{\Gamma_{S-D}\lambda_y}{4} \right) \right]^{-N_r} \tag{23}$$

where $\lambda_y$ are the nonzero eigenvalues of the matrix $\tilde{\mathbf{A}}$ defined in (12). At high SNR, using (21) and (23), we get the approximate upper bound for PEP as follows,

$$p_{UB}^{S-D}(d_1,\chi,M) \approx$$

$$\left[ \frac{1}{2^K K} \sum_{k=1}^{K} \sum_{b=0}^{1} \sum_{\mathbf{X}_S \in \chi_b^k} \sum_{\mathbf{Z}_S \in \chi_{\bar{b}}^k} \left( \prod_{y=1}^{\rho} \left( 1 + \frac{\Gamma_{S-D}\lambda_y}{4} \right) \right)^{-N_r} \right]^{d_1}$$

$$= \left[ \frac{4}{\Gamma_{S-D}\Lambda_S^2} \right]^{\rho N_r d_1} \tag{24}$$

where,

$$\Lambda_S^2(\chi, M, N_r) \triangleq$$

$$\left[ \frac{1}{2^K K} \sum_{k=1}^K \sum_{b=0}^1 \sum_{\mathbf{X}_S \in \chi_b^k} \sum_{\mathbf{Z}_S \in \chi_{\bar{b}}^k} \left( \prod_{y=1}^\rho (\lambda_y) \right)^{-N_r} \right]^{-1/\rho N_r}. \quad (25)$$

In logarithmic domain, the (25) can be written as,

$$\log_{10} P_b \simeq -\frac{\rho N_r d_f}{10} \left[ (R\Lambda_S^2)_{\mathrm{dB}} + (\Gamma_{S-D})_{\mathrm{dB}} \right] + c \quad (26)$$

where $c$ is any constant. It should be noted that the difference between BI-BoCM-ID and BI-BoCM is only a horizontal shift at EF region, latter is assumed in this paper. For large values of $E_b/N_0$ defined as SNR per bit, the BER curve on a log-scale is a straight line with a slope proportional to the overall diversity order $\rho N_r d_f$, which is a direct function of $d_f$, in other words, the diversity order significantly depends on the minimum distance of a binary code (convolutional, turbo or LDPC). The factor $(R\Lambda_S^2)_{\mathrm{dB}}$ in (26) shifts the BER curve horizontally towards the left, and shows the coding gain.

## 6.2  Coded-Cooperative Scheme with Labeling Diversity, (BI-BoDTCM)

In case of coded-cooperative scheme with labeling diversity, i.e., BI-BoDTCM, the PEP in (20) becomes the joint PEP of the $S-D$ link and the $R-D$ link, i.e., $p_{UB}^{S-D}(d_1, \chi, M)$ and $p_{UB}^{R-D}(d_2, \chi, M)$, respectively. Mathematically,

$$p_{UB}(d, \chi, M) = p_{UB}^{S-D}(d_1, \chi, M) p_{UB}^{R-D}(d_2, \chi, M) \quad (27)$$

where $d = d_1 + d_2$ is the Hamming distance of the codeword jointly constructed by the source and the relay nodes. Since, the transmitter at the relay is identical to the one used at the source, hence, all the approximations assumed for deriving (24) for non-cooperative scenario still hold true for the coded-cooperative scenario and (27) becomes,

$$p_{UB}(d, \chi, M) \approx p_{UB}^{S-D}(d_1, \chi, M) p_{UB}^{R-D}(d_2, \chi, M)$$

$$= \left[ \frac{1}{2^K K} \sum_{k=1}^K \sum_{b=0}^1 \sum_{\mathbf{X}_S \in \chi_b^k} \sum_{\mathbf{Z}_S \in \chi_{\bar{b}}^k} \left( \prod_{y=1}^\rho \left( 1 + \frac{\Gamma_{S-D}\lambda_y}{4} \right) \right)^{-N_r} \right]^{d_1}$$

$$\times \left[ \frac{1}{2^K K} \sum_{k=1}^K \sum_{b=0}^1 \sum_{\mathbf{X}_R \in \chi_b^k} \sum_{\mathbf{Z}_R \in \chi_{\bar{b}}^k} \left( \prod_{y=1}^\rho \left( 1 + \frac{\Gamma_{R-D}\lambda_y}{4} \right) \right)^{-N_r} \right]^{d_2}$$

$$(28)$$

where $\mathbf{X}_R$ is a transmitted codeword at the relay and $\mathbf{Z}_R$ is the received codeword with errors at the destination during the second time slot. (28) is further simplified using (24) as,

$$p_{UB}(d, \chi, M) \approx \left[ \left( \frac{4}{\Gamma_{S-D}\Lambda_S^2} \right)^{d_1} \left( \frac{4}{\Gamma_{R-D}\Lambda_R^2} \right)^{d_2} \right]^{\rho N_r}. \quad (29)$$

The average error probability $P_b$ of the BI-BoDTCM scheme can be determined by substituting $p_{UB}(d, \chi, M)$ from (29) in (19). The diversity order of the coded-cooperative scheme is $\rho N_r(d_1 + d_2)$ and the full diversity is achieved when $d_1 \neq 0$ and $d_2 \neq 0$. It should be noted that for the fast fading, performance of the coded-cooperative scheme is identical to the performance of the non-cooperative scheme especially when the source and the relay have identical channel statistics, i.e., $\Gamma_{R-D} = \Gamma_{S-D}$. However, for dissimilar channel characteristics, i.e., $\Gamma_{R-D} \neq \Gamma_{S-D}$, where $\Gamma_{R-D} > \Gamma_{S-D}$ there is a definite BER performance improvement for a coded-cooperative scheme, also shown later in the simulation section.

# 7.  Joint Iterative Decoding Schemes

In this section, we briefly discuss joint iterative decoding schemes employed for bit-interleaved distributed space-time turbo and LDPC codes with and without labeling diversity.

## 7.1  Joint Parallel Iterative Decoding for DTC

The joint parallel iterative decoding scheme is shown in Fig. 7, [9], is primarily based on the decoding configuration shown in Fig. 5. The dashed line shows the reception of the data from relay node during the second time slot. The pseudo-random bit interleavers (PRI) used at the source and at the relay are represented as $\pi_{source}, \pi_{relay}$, respectively, also shown in Fig. 7. To improve the free distance of a distributed turbo code, $S$-random interleaver $\pi_S$ is used at the relay, where $S \leq \sqrt{K/2}$. During the first time slot, the space-time demapper outputs its extrinsic LLRs $\lambda_{dem}^e$, which are soft decisions related to the systematic bits and the parity bits transmitted at the source. This $\lambda_{dem}^e$ is further sent to the de-interleaver $\pi_{source}^{-1}$ corresponding to the bit-interleaver used at the source $\pi_{source}$. These de-interleaved LLRs are then de-multiplexed into LLRs for the systematic and the parity bits such as $\lambda_s$ and $\lambda_{p_1}$. The SISO RSC decoder 1 takes these LLRs and generates its extrinsic information for the received parity and systematic bits $\mu_{p_1}^{[dec1,e]}$ and $\mu_{S12}$, respectively. The extrinsic information for the systematic bit $\mu_{S12}$ is $S$-random interleaved and passed to the second SISO decoder.

During the second time slot, the space-time demapper receives the signal from the relay and outputs its extrinsic LLRs for the second parity bits $\mathbf{p}_2$, which is de-interleaved ($\pi_{relay}^{-1}$) corresponding to the bit-interleaver $\pi_{relay}$ used at the relay. The de-interleaved parity bit LLRs $\lambda_{p_2}$ are then passed to the second SISO decoder. The second SISO decoder also generates the extrinsic LLRs for the second set of parity bits $\mu_{p_2}^{[dec2,e]}$ and the systematic bits $\mu_{S21}$, which are de-interleaved ($\pi_S^{-1}$) and feedback to the first SISO decoder. The exchange of extrinsic information for the systematic bit between the two SISO decoders takes place for desired number of iterations and finally, the systematic bits from the sec-
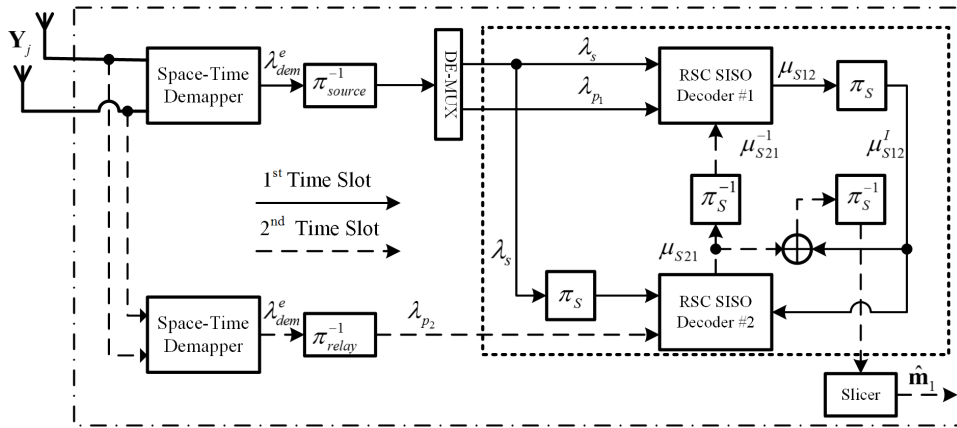
**Fig. 7.** Joint parallel iterative decoding for BI-BoDTCM with reference to time.

ond SISO decoder are de-interleaved $(\pi_S^{-1})$ and passed to the slicer for hard decisions on the measured LLRs.

## 7.2 Joint Min-Sum Iterative Decoding for Distributed Space-Time LDPC Codes

The received signal is first passed to the soft demodulator, which generates the LLRs $\lambda_{dem}^e$ for each received bit. These LLRs are further de-interleaved by $\pi_{soruce}^{-1}$ and passed to the iterative joint min-sum iterative decoder that is primarily based on the bilayer Tanner graph as shown in Fig. 2 . During each iteration, the extrinsic information resulting from the variable and check nodes in the bilayer Tanner graph is exchanged. Furthermore, joint decoding of the two received signals from the source and the relay results in increased coding gains as compared to the individual decoding of the received signals, also shown in [31]. The details of this joint min-sum decoding are skipped here for brevity and interested reader is referred to [31].

# 8. Numerical Results

This section presents the numerical results for proposed encoding schemes in aforementioned sections. Three different types of space-time channel codes such as convolutional, turbo and LDPC codes are used in conjunction with labeling diversity. Therefore, this section is divided in three sub-sections to analyse the effect of labeling diversity for each channel code individually. The simulation parameters common to all the three channel codes are: perfect channel state information (CSI) is assumed at all receiving nodes. Each communication node has two transmit and two receive antennas, i.e., $N_t = N_r = 2$, moreover, each node communicates in half-duplex mode. The optimal labeling maps used to provide labeling diversity are shown in Fig. 6, and for non-labeling diversity (NLD), Gray labeling is used as a benchmark comparison. Rayleigh fading channel is assumed among all nodes assuming that the fading coefficient remains constant for the duration of one space-time codeword and may change independently over the transmission of next space-time codeword.
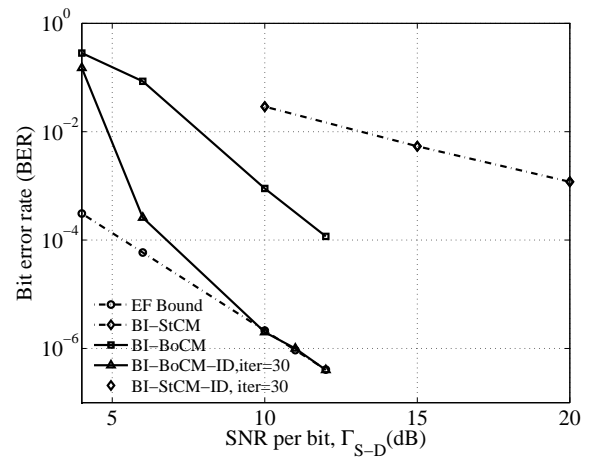


**Fig. 8.** Comparison of space-time convolutional codes with and without labeling diversity, $R_c = 0.5$.

## 8.1 Convolutional Codes

At first, we present the BER performance of the convolutional codes as shown in Fig. 8. The generator matrix of the convolutional code is $g = [1, 5/7]_8$, in an octal form, information block size $K = 120$ bits and $R_c = 0.5$. Since, original BI-BoCM was presented with iterative decoding i.e., BI-BoCM-ID therefore we also present the performance of BI-BoCM-ID in comparion with BI-StCM-ID. It can be seen that both BI-BoCM and BI-BoCM-ID completely outperform the BI-StCM and BI-StCM-ID schemes with BER performance gains more than 10 dB at BER $\approx 10^{-4}$. The BER performance gain is more significant in case of iterative demodulator and soft-input and soft-output (SISO) decoder and approaches theoretical EF bound derived in (24). However, the penalty is the overall latency of the system, which may not be a feasible solution for most of the real time applications, hence, we restrict our analysis only to the BI-BoCM schemes.

## 8.2 Space-Time Turbo Codes

In this subsection, we consider space-time turbo codes with and without labeling diversity in both coded-cooperative and non-cooperative scenarios. The generator

matrix of both RSC encoders used at the source and at the relay is $g = [1, 5/7]_8$, in an octal form, and the size of $S$−random interleaver is 120 bits, $S$−constraint length equal to 7. The number of log-MAP decoder iterations are five. The turbo code is punctured to make the code rate $R_c = 0.5$. The BER performances of BI-StTCM and BI-BoTCM are shown in Fig. 9, where, BI-BoTCM completely outperforms the BI-StTCM. Moreover, the theoretical EF bound derived in (24) is also validated by the help of numerical simulations.

Next, we analyse coded-cooperative space-time turbo codes with and without labeling diversity. From Fig. 10, it is observed that BI-BoDTCM outperforms BI-StDTCM scheme again with a significant margin. It is assumed that relay has an additional gain of 2 dB as compared to the source i.e., $\Gamma_{R-D} = \Gamma_{S-D} + 2$dB.

Further, comparing Fig. 9 and Fig. 10, it can be seen that the BI-BoDTCM (coded-cooperative) also outperforms the BI-BoTCM (non-cooperative) scheme and the BER performance curve converges more rapidly to the EF performance bound derived in 29.

Further in Fig. 11, we present the BER performance comparison of BI-BoDTCM and BI-StDTCM schemes for the most *practical* scenario, i.e., non-ideal S-R channel ($\Gamma_{S-R} \neq \infty$). We assume that the link between the source and the relay node is at $\Gamma_{S-R} = 10$ dB, and from Fig. 11 it is observed that the BI-BoDTCM clearly outperforms BI-StDTCM as the BER curve for BI-StDTCM becomes flat. This flattening of the BER curve is because the relay is in *outage* and there is no coded-cooperation between the source and the relay nodes. Usually in such scenarios, cyclic redundancy check (CRC) is employed at the relay to avoid error propagation at the relay which leads to erroneous decoding at the destination and results in BER curve flattening [6]. The BER performance of BI-BoDTCM with $\Gamma_{S-R} = 10$ dB is only 0.2 dB away from its BER performance for an ideal $S-R$ channel, i.e., $\Gamma_{S-R} = \infty$ dB, which shows the effectiveness of labeling diversity in the coded-cooperative scenarios.

## 8.3 Space-Time LDPC Codes

In this subsection, we consider LDPC codes for the proposed encoding schemes. At first, we consider non-cooperative scenario with and without labeling diversity. The parameters of LDPC code used are: $d_v = 2$ and $d_c = 4$, where $d_v$ is number of 1's in columns and $d_c$ is number of 1's in rows of a parity check matrix **H** and the code rate is $R_c = 0.5$. From Fig. 12, it can be seen that the BI-BoLCM clearly outperforms BI-StLCM under identical conditions. Moreover from Fig. 12 it is observed that for longer length LDPC codes i.e., $K = 1000, N = 2000$ the coding gain for BI-BoLCM is further improved by approximately 7dB at BER$\approx 10^{-6}$ as compared to short length LPDC codes, which encourages use of longer length LDPC codes, obviously at increased decoding complexity. Furthermore, the longer length LDPC codes also lowers the EF region.
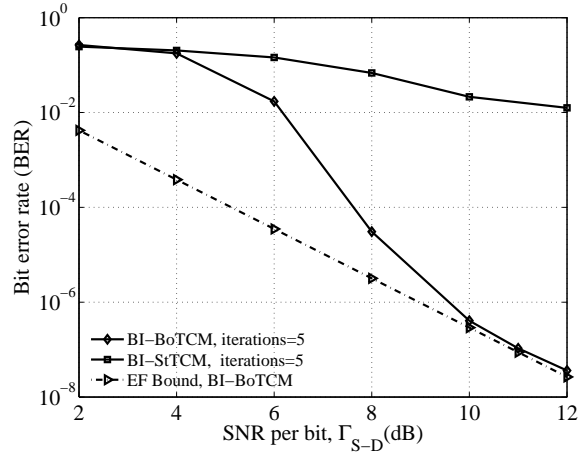


**Fig. 9.** Comparison of non-cooperative space-time turbo codes with and without labeling diversity, $R_c = 0.5$.
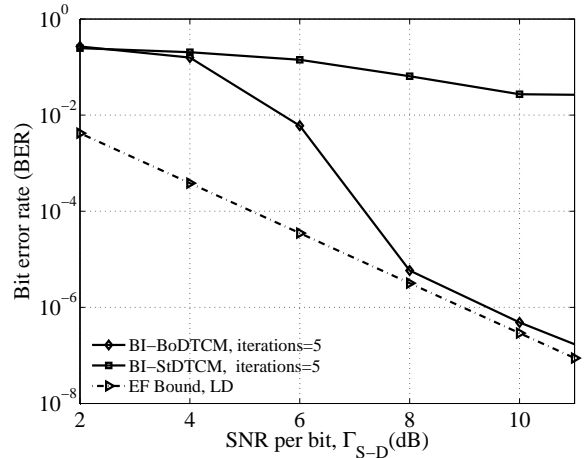


**Fig. 10.** Comparison of coded-cooperative space-time turbo codes with and without labeling diversity, $R_c^o = 0.5$, $\Gamma_{R-D} = \Gamma_{S-D} + 2$dB.
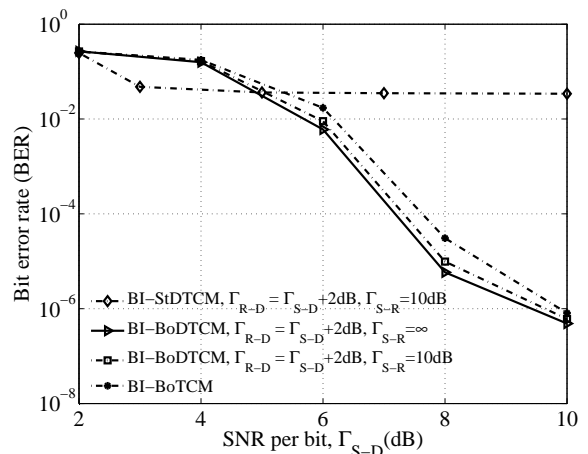


**Fig. 11.** BER performance comparison among different coded-cooperative scenarios where S-R link condition varies as $\Gamma_{S-R} = \infty, 10$ dB, and $\Gamma_{R-D} = \Gamma_{S-D} + 2$ dB. The non-cooperative scheme (with turbo code of $R_c = 0.5$ and labeling diversity) acts as an upper bound on the BER performance of BI-BoDTCM. Moreover, code rate for coded-cooperative scheme is $R_c^o = 0.5$.
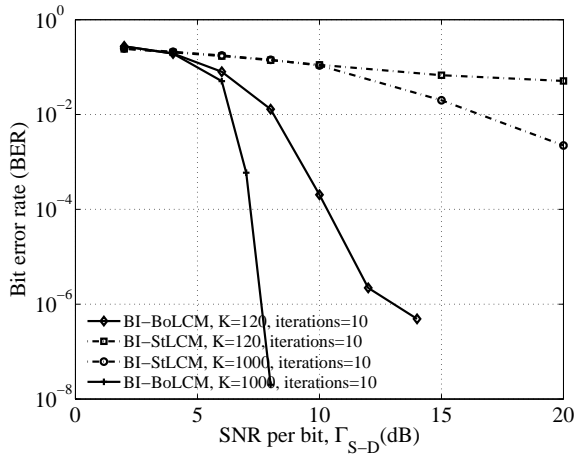
**Fig. 12.** Comparison of short and longer length non-cooperative space-time LDPC codes with and without labeling diversity, $R_c = 0.5$.
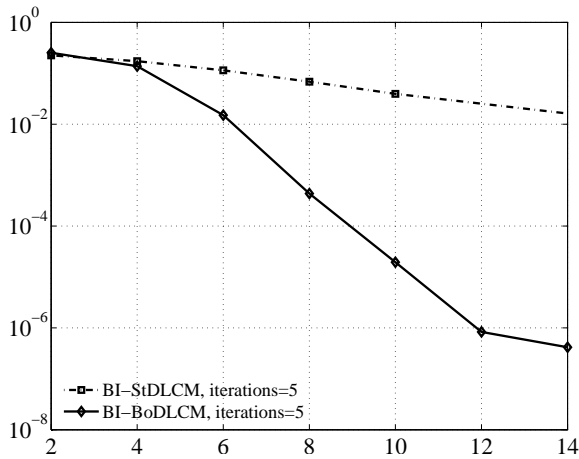


**Fig. 13.** Comparison of coded-cooperative space-time LDPC codes with and without labeling diversity, $R_c^o = 0.5$, $\Gamma_{R-D} = \Gamma_{S-D} + 2$ dB.

Finally, we consider distributed LPDC (DLDPC) codes with and without labeling diversity. For DLDPC codes, the fundamental simulation parameters are same as in case of non-cooperative case i.e., $d_v = 2$ and $d_c = 4$, for both $\mathbf{H}_S$ and $\mathbf{H}_R$ parity check matrices used at the source and at the relay, respectively. Moreover, the overall code rate $R_c^o = 0.5$ is also identical to code rate as in case of non-cooperative case. The relay has an additional 2 dB gain relative to the source i.e., $\Gamma_{R-D} = \Gamma_{S-D} + 2$ dB. Again, it is observed from Fig. 13 that BI-BoDLDPC outperforms the BI-BoLDPC under identical conditions.

# 9. Conclusions

In this paper, different space-time channel codes such as convolutional, turbo and LDPC codes are analyzed with state-of-the-art labeling diversity scheme. Coded-cooperative schemes in conjunction with labeling diversity clearly outperforms the non-cooperative schemes. Theoretical bounds for bit error rate performance at EF region for coded-cooperative schemes are derived and verified with the help of numerical simulations. The effect of labeling diversity is also illustrated for non-ideal $S - R$ channels (practical scenario), where the relay outage probability is considerably lowered as compared to the coded-cooperative scheme without any labeling diversity.

# Acknowledgments

# References

[1] VAN DER MEULEN, E. C. Three-terminal communication channels. *Advances in Applied Probability*, 1971, vol. 3, no. 1, p. 120–154.

[2] LANEMAN, J. N., TSE, D. N. C., WORNELL, G. W. Cooperative diversity in wireless networks: Efficient protocols and outage behavior. *IEEE Transactions on Information Theory*, 2004, vol. 50, no. 12, p. 3062–3080. DOI: 10.1109/TIT.2004.838089

[3] SENDONARIS, A., ERKIP, E., AAZHANG, B., User cooperation diversity. Part I. System description. *IEEE Transactions on Communications*, 2003, vol. 51, no. 11, p. 1927–1938. DOI: 10.1109/TCOMM.2003.818096

[4] ALAMOUTI, S. A simple transmit diversity technique for wireless communications. *IEEE Journal on Selected Areas in Communications*, 1998, vol. 16, no. 8, p. 1451-1458. DOI: 10.1109/49.730453

[5] HUNTER, T. E., NOSRATINIA, A. Cooperation diversity through coding. In *Proceedings of IEEE International Symposium on Information Theory*. Lausanne (Switzerland), 2002, p. 220. DOI: 10.1109/ISIT.2002.1023492

[6] HUNTER, T. E., NOSRATINIA, A. Diversity through coded cooperation. *IEEE Transactions on Wireless Communications*, 2006, vol. 5, no. 2, p. 283–289. DOI: 10.1109/TWC.2006.1611050

[7] ZHAO, B., VALENTI, M. C. Distributed turbo coded diversity for relay channel. *Electronics Letters*, 2003, vol. 39, no. 10, p. 786–787. DOI: 10.1049/el:20030526

[8] VALENTI, M. C., ZHAO, B. Distributed turbo codes: towards the capacity of the relay channel. In *IEEE 58th Vehicular Technology Conference (VTC 2003-Fall)*. Orlando (FL, USA), 2003, vol. 1, p. 322–326. DOI: 10.1109/VETECF.2003.1285032

[9] EJAZ, S., YANG, F.-F. Turbo codes with modified code matched interleaver for coded-cooperation in half-duplex wireless relay networks. *Frequenz*, 2015, vol. 69, no. 3-4, p. 171–184. DOI: 10.1515/freq-2014-0072

[10] CHAKRABARTI, A., DE BAYNAST, A., SABHARWAL, A., AAZHANG, B. Low density parity check codes for the relay channel. *IEEE Journal on Selected Areas in Communications*, 2007, vol. 25, no. 2, p. 280–291. DOI: 10.1109/JSAC.2007.070205

[11] HU, J., DUMAN, T. M. Low density parity check codes over wireless relay channels. *IEEE Transactions on Wireless Communications*, 2007, vol. 6, no. 9, p. 3384–3394. DOI: 10.1109/TWC.2007.06083

[12] BRAVO-SANTOS, A. Polar codes for the Rayleigh fading channel. *IEEE Communications Letters*, 2013, vol. 17, no. 12, p. 2352–2355. DOI: 10.1109/LCOMM.2013.111113.132103

[13] ZHAN, Q., DU, M., WANG, Y., ZHOU, F. Half-duplex relay systems based on polar codes. *IET Communications*, 2014, vol. 8, no. 4, p. 433–440. DOI: 10.1049/iet-com.2013.0521

[14] GENC, F., RESAT, M. A., SAVASCIHABES, A., ERTUG, O. On the comparative performance analysis of turbo-coded non-ideal sigle-carrier and multi-carrier waveforms over wideband Vogler-Hoffmeyer HF channels. *Radioengineering*, 2014, vol. 23, no, 3, p. 872–879.

[15] CAIRE, G., TARICCO, G., BIGLIERI, E. Bit-interleaved coded modulation. *IEEE Transactions on Information Theory*, 1998, vol. 44, no. 3, p. 927–946. DOI: 10.1109/18.669123

[16] HUANG Y., RITCEY J. A. Optimal constellation labeling for iteratively decoded bit-interleaved space-time coded modulation. *IEEE Transactions on Information Theory*, 2005, vol. 51, no. 5, p. 1865–1871. DOI: 10.1109/TIT.2005.846409

[17] CLEVORN, T., GODTMANN, S., VARY, P. Optimized mappings for iteratively decoded BICM on Rayleigh channels with interleaving. In *IEEE 63$^{rd}$ Vehicular Technology Conference (VTC 2006-Spring)*. Melbourne (Australia), 2006, p. 2083–2087. DOI: 10.1109/VETECS.2006.1683223

[18] KRASICKI, M. Improved labelling diversity for iteratively-decoded multi-antenna systems. In *IEEE 7$^{th}$ International Wireless Communications and Mobile Computing Conference (IWCMC)*. Istanbul (Turkey), 2011, p. 359–364. DOI: 10.1109/IWCMC.2011.5982560

[19] RUMANEK, J., SEBESTA, J. New channel coding methods for satellite communication. *Radioengineering*, 2010, vol. 19, no. 1, p. 155–161.

[20] KRASICKI, M. Labeling diversity for MIMO systems. *11$^{th}$ European Wireless Conference-Sustainable Wireless Technologies (European Wireless)*. Vienna (Austria), 2011, p. 1–7.

[21] KRASICKI, M., Essence of 16-QAM labelling diversity. *Electronics Letters*, 2013, vol. 49, no. 8, p. 567–569. DOI: 10.1049/el.2012.4275

[22] KRASICKI, M. Algorithm for generating all optimal 16-QAM BI-STCM-ID labelings. *Wireless Personal Communications*, 2015, p. 1–22. DOI: 10.1007/s11277-015-2431-1

[23] KRASICKI, M., SZULAKIEWICZ, P. Boosted space-time diversity scheme for wireless communications. *Electronics Letters*, 2009, vol. 45, no. 16, p. 843–845. DOI: 10.1049/el.2009.1052

[24] ABRAMOVICI, I., SHAMAI, S. On turbo encoded BICM. *Annales Des Telecommunications*, 1999, vol. 54, no. 3–4, p. 225–234. DOI: 10.1007/BF02998584.

[25] BURR, A., HIRST, S. FER bounds and estimates for bit-interleaved space-time turbo-codes. In *4$^{th}$ International Symposium on Turbo Codes &Related Topics; 6$^{th}$ International ITG-Conference on Source and Channel Coding (TURBOCODING)*. Munich (Germany), 2006, p. 1-6.

[26] TAROKH, V., SESHADRI, N., CALDERBANK, A. R. Space-time codes for high data rate wireless communication: Performance criterion and code construction. *IEEE Transactions on Information Theory*, 1998, vol. 44, no. 2, p. 744–765. DOI: 10.1109/18.661517

[27] WANG, Y., XIE, L., CHEN, H., WANG, K. Improved decoding algorithm of bit-interleaved coded modulation for LDPC code. *IEEE Transactions on Broadcasting*, 2010, vol. 56, no. 1, p. 103–109. DOI: 10.1109/TBC.2009.2036950

[28] ZHANG, R., BIE, Z. Optimality analysis of bit-interleaved LDPC coded modulation schemes. In *Global Mobile Congress (GMC)*. Shanghai (China), 2010, p. 1–5. DOI: 10.1109/GMC.2010.5634560

[29] XIE, Q., PENG, K., SONG, J., YANG, Z. Bit-interleaved LDPC-coded modulation with iterative demapping and decoding. In *IEEE 69$^{th}$ Vehicular Technology Conference (VTC 2009-Spring)*. Barcelona (Spain), 2009, p. 1–5. DOI: 10.1109/VETECS.2009.5073425

[30] LU, B., WANG, X., NARAYANAN, K. R. LDPC-based space-time coded OFDM systems over correlated fading channels: Performance analysis and receiver design. *IEEE Transactions on Communications*, 2002, vol. 50, no. 1, p. 74–88. DOI: 10.1109/26.975756

[31] ZHANG, S., YANG, FF., TANG, L., MAHARAJ, B. LDPC-coded cooperation with receive multi-antenna and unknown CSI in the destination. *Wireless Personal Communications*, 2013, vol. 72, no. 4, p. 2685–2703. DOI: 10.1007/s11277-013-1174-0

[32] RAZAGHI, P., YU, W. Bilayer low-density parity-check codes for decode-and-forward in relay channels. *IEEE Transactions on Information Theory*, 2007, vol. 53, no. 10, p. 3723–3739. DOI: 10.1109/TIT.2007.904983

# About the Authors ...

**Saqib EJAZ** received his B.Sc. (Hons.) degree in Electrical engineering from the University of Engineering and Technology, Taxila, Pakistan, in 2006. Later, he did his M.S. degree at Ghulam Ishaq Khan Institute of Engineering sciences and technology (GIKI), KPK, Pakistan, in 2008. Since 2012, he has been a Ph.D. candidate at College of Electronic and Information Engineering, Nanjing University of Aeronautics and Astronautics, China. His research interests include information theory, channel coding, multi-input, and multi-output systems, cooperative diversity, and coded-modulation techniques.

**FengFan YANG** received the B.Sc., M.Sc., and Ph.D. degrees from Nanjing University of Aeronautics and Astronautics, Nanjing, Northwestern Polytechnical University, and Southeast University in 1990, 1993, and 1997 from P. R. China, respectively, all in Electronic Engineering. He has been with College of Information Science and Technology, Nanjing University of Aeronautics and Astronautics since May 1997. From October 1999 to May 2003, he was a research associate at Centre for Communication Systems Research, University of Surrey, UK, and Department of Electrical and Computer Engineering (ECE), McGill University, Canada. His major research interests are information theory and channel coding, especially iteratively decodable codes, such as turbo codes and LDPC codes, and their applications for mobile and satellite communications.

**HongJun XU** (MIEEE, 07) received the B.Sc. degree from the University of Guilin Technology, Guilin, China, in 1984; the M.Sc. degree from the Institute of Telecontrol and Telemeasure, Shi Jian Zhuang, China, in 1989; and the Ph.D. degree from the Beijing University of Aeronautics and Astronautics, Beijing, China, in 1995. From 1997 to 2000, he was a Postdoctoral Fellow with the University of Natal, Durban, South Africa, and Inha University, Incheon, Korea. He is currently a Professor with the School of Engineering, University of KwaZulu-Natal, Durban. He is the author of more than 20 journal papers. His research interests include wireless communications and digital systems.